ADVANCED FUNCTIONAL MATERIALS
www.afm-journal.de

Materials Views
www.MaterialsViews.com

Topological-Structure Modulated Polymer Nanocomposites Exhibiting Highly Enhanced Dielectric Strength and Energy Density

Penghao Hu, Yang Shen, Yuhan Guan, Xuehui Zhang, Yuanhua Lin, Qiming Zhang,* and Ce-Wen Nan*

Dielectric materials with high electric energy densities and low dielectric losses are of critical importance in a number of applications in modern electronic and electrical power systems. An organic–inorganic 0–3 nanocomposite, in which nanoparticles (0-dimensional) are embedded in a 3-dimensionally connected polymer matrix, has the potential to combine the high breakdown strength and low dielectric loss of the polymer with the high dielectric constant of the ceramic fillers, representing a promising approach to realize high energy densities. However, one significant drawback of the composites explored up to now is that the increased dielectric constant of the composites is at the expense of the breakdown strength, limiting the energy density and dielectric reliability. In this study, by expanding the traditional 0–3 nanocomposite approach to a multilayered structure which combines the complementary properties of the constituent layers, one can realize both greater dielectric displacement and a higher breakdown field than that of the polymer matrix. In a typical 3-layer structure, for example, a central nanocomposite layer of higher breakdown strength is introduced to substantially improve the overall breakdown strength of the multilayer-structured composite film, and the outer composite layers filled with large amount of high dielectric constant nanofillers can then be polarized up to higher electric fields, hence enhancing the electric displacement. As a result, the topological-structure modulated nanocomposites, with an optimally tailored nanomorphology and composite structure, yield a discharged energy density of 10 J/cm^3 with a dielectric breakdown strength of 450 kV mm^{-1}, much higher than those reported from all earlier studies of nanocomposites.

1. Introduction

Dielectric materials with high dielectric constant (ε_r), high breakdown strength (E_b), low dielectric loss, and hence high electric energy density (U_e), are of critical importance in a number of the modern electronics and electrical power systems, such as hybrid electric vehicles (HEV), medical defibrillators, and power regulations in smart grid.[1,2] Currently, the dielectric materials of choice for energy storage are neat polymers, such as biaxially oriented polypropylene (BOPP), due largely to their high breakdown strength. Nevertheless, these state-of-art dielectric polymers suffer from the low dielectric constant ($\varepsilon_r < 3$), limiting the energy density and hence their applications.[3–5]

In general, the U_e of a dielectrics is $U_e = \int E\,dD$, which indicates that the electric displacement (D) and the breakdown strength have to be enhanced simultaneously in order to realize high energy density. Polymer nanocomposites represent a promising approach, which has the potential of combining the high E_b of the polymer matrix with the high ε_r of the ceramic fillers to realize high energy density and have been investigated extensively in the past.[6–14] However, one significant

Dr. P. H. Hu, Prof. Y. Shen, Y. H. Guan, Dr. X. H. Zhang, Prof. Y. H. Lin, Prof. C.-W. Nan
School of Materials Science and Engineering
State Key Lab of New Ceramics and Fine Processing
Tsinghua University
Beijing 100084, China
E-mail: shyang-mse@tsinghua.edu.cn
Dr. P. H. Hu
School of Chemical and Biological Engineering
University of Science and Technology Beijing
Beijing 100083, China
Prof. Q. M. Zhang
Department of Electrical Engineering
and Materials Research Institute
The Pennsylvania State University
University Park
PA 16802, USA
E-mail: qxz1@psu.edu

DOI: 10.1002/adfm.201303684

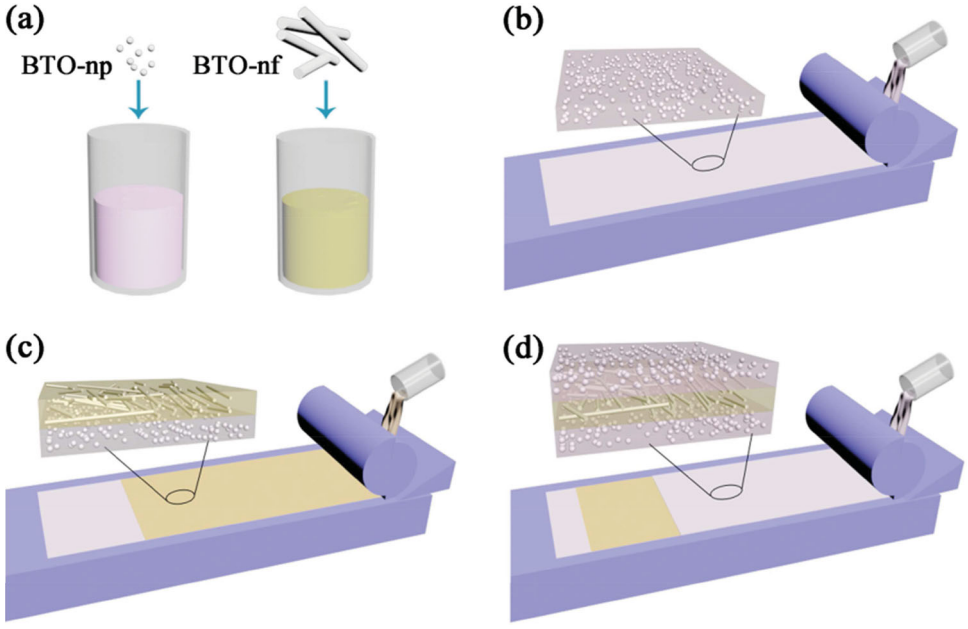

Figure 1. Schematic drawing of the approach of layer-by-layer casting for the fabrication of the sandwich multilayer films. (a) Nanofillers were dispersed in the PVDF suspension, (b) one layer with BTO-np was cast, (c) the central layer with BTO-nf was cast, (d) the other layer with BTO-np was cast.

drawback of the composites explored up to now is that the increased dielectric constant of the composites is at the expense of the significant reduction of the breakdown strength. It is worth noting that the most promising polymer nanocomposites studied so far are these considered as 0–3 type composites (zero-dimensional fillers (nanoparticles) in a three-dimensionally connected polymer matrix), which have limited variables that can be tailored to enhance both the electrical displacement and dielectric strength. In this contribution, we show that by expanding the traditional 0–3 nanocomposite approach to a multilayered structure, as illustrated in **Figure 1**, we can achieve both enhanced electrical displacement as well as a higher breakdown field than that of the polymer matrix. Such a topological-structure nanocomposite (for example, a three layer composite as shown in Figure 1) combines synergistically the complementary properties of the constituent layers. That is, a central layer of higher breakdown strength is introduced in the breakdown path which can substantially improve the overall breakdown strength of the multilayer-structured composite film, and the outer composite layers filled with large amount of high ε_r nanometric fillers can then be polarized up to higher electric field, hence enhancing the electric displacement. As will be shown in the paper, the topological-structure modulated nanocomposites with optimally tailored nanomorphology and composite structure yield a discharged energy density near 10 J/cm^3 with a dielectric breakdown strength at 450 kV/mm, much higher than these reported from all earlier studies of 0–3 nanocomposites.[18,19]

The fundamental reason for the reduction of the breakdown strength in the traditional 0–3 composites is the large differences between the "dielectric hard (low ε_r)" polymer and the "dielectric soft (high ε_r)" ceramic fillers that result in severe local electric field concentration in the polymer matrices, causing significant reduction of the overall breakdown strength of polymer composites, as shown by Li et al., based on effective medium analysis,[15] and by Kim et al., within the framework of self-consistent effective medium theory which has been experimentally verified in the $BaTiO_3$-filled polymer nanocomposites.[16] Besides limiting the energy density of the composite dielectrics, the lowering of breakdown strength also reduces the capacitor device reliability. Hence, it is of great interest while also a challenge to create approaches to significantly enhance the breakdown strength of composites containing high ε_r fillers for higher dielectric constant.

During past decade, a large number of ideas have sought to mitigate the local field concentration in the composites and hence improve the breakdown strength. One effective approach is to employ "high dielectric permittivity" polymer matrix that approaches the dielectric permittivity of the fillers. For instance, Wang et. al., achieved much enhanced energy density, through the interfacial effects in nanocomposites, by using P(VDF-TrFE-CTFE) (ε_r ~ 42) as polymer matrix and TiO_2 nanorods (ε_r ~ 47) as fillers.[17] Another method is to introduce interfacial buffer layers between the polymer matrix and ceramic fillers and modify the interfacial modulus, as proposed by Tanaka et al.[18] This approach was then systematically investigated by Fredin et al.,[19] in Polypropylene-based nanocomposites filled with several kinds of metal and oxide nanoparticles, where Al_2O_3 surface layers of different thickness were coated on the nanoparticles by in-situ catalytic encapsulation. The Al_2O_3 surface layers of moderate dielectric permittivity suppressed leakage current and reduced dielectric loss, yielding an enhanced energy density and improved breakdown strength, as compared with the nanocomposites with bare nanofillers. Here we expand the composite concept further by integrating synergistically different composite layers with complementary properties into topological-structure modulated composites which lead to the enhancement in both the electric displacement and dielectric strength of the composites.

In this study, $BaTiO_3$ nanoparticles (BTO-np) were used as the nanometric fillers in the outer composite layers to induce high electric constant, while $BaTiO_3$ nanofibers (BTO-nf) were introduced in the central composite layer for improving the breakdown strength. Polyvinylidene difluoride (PVDF) was employed as the polymer matrix which has a dielectric constant $\varepsilon_r \sim 7$. Recent phase-field modeling[20] and experimental results[21–24] all indicate that the orientation of large-aspect-ratio fillers perpendicular to the direction of external electric field is favorable for mitigating local field concentration and leads to higher breakdown strength. Indeed, it was observed that the nanocomposites with 2% volume fraction of BTO-nf with nanofibers long axis aligned preferably in parallel to the film surface direction exhibited an E_b 34% higher than that of the polymer matrix, which is distinctively different from that of the nanocomposites with random nanofillers distribution. Moreover, by tailoring the nanocomposite topological structure shown in Figure 1 to the optimal, both the energy density and the dielectric strength can be significantly enhanced concomitantly, i.e., an E_b of more than 175% of and a discharged energy density $U_{dis} = 9.72$ J/cm^3 which is more than 260% of that of the polymer matrix can be achieved. The results demonstrate the promise of the topological structure nanocomposite approach, in which the hetero-layer structure along the external electric field direction effectively increases the dielectric breakdown strength while the layers with high loading of high dielectric constant fillers enhance the energy density.

2. Results and Discussion

The sandwich-structured composite films were fabricated by a layer-by-layer tape casting method at room temperature, as illustrated schematically in Figures 1(a–c), which could control each layer thickness to 1 μm. In order to properly design the topological-structured nanocomposite films, the PVDF-based composite films with 0~30 vol% of BTO-np and with 0~5 vol% of BTO-nf were prepared separately and their dielectric properties were investigated. Both BTO-np and BTO-nf could be dispersed homogeneously in the PVDF matrices without large agglomeration, as revealed by the SEM images (Figure S1 in Supporting Information). As shown in **Table 1**, the dielectric permittivity increases with the nanofillers in both of the nanocomposites with BTO-np and BTO-nf (see also Figure S2 in the Supporting Information). However, in composites with BTO-np, the E_b continuously decreases from 258 kV/mm for the PVDF matrix to 174 kV/mm for the composites with 30 vol% of BTO-np and is always lower than that of the matrix, which is consistent with earlier works.[15,16] In contrast, the nanocomposite with 2 vol% of BTO-nf with preferred orientations of fibers in perpendicular to the applied field direction (see Figure S1(c) in the Supporting Information) exhibits a breakdown field of 347 kV/mm, higher than that of the polymer matrix. Further introduction of the BTO-nf leads to decrease in E_b. The discharged energy densities of the composite films derived from the *D*–*E* loops are also presented in Table 1. For the BTO-np/PVDF composites, despite the largely increased dielectric constants, the discharged energy densities are compromised by the decrease in E_b and increased conduction loss which reaches a maximum of 4.23 J/cm^3 for the composite with 10 vol% of BTO-np. In contrast, the maximal discharged energy density for composites with BTO-nf is higher, 5.86 J/cm^3, due to higher E_b for the nanocomposite with 2 vol% of BTO-nf.

Table 1. Dielectric constants, breakdown strength, and discharged energy density of the PVDF-based single layer film with different BTO-nf and BTO-np loadings.

Composite	ε at 1 kHz	E_b [kV/mm]	U_{dis} [J/cm^3]
PVDF	6.90	258	3.70
5 vol% BTO-np	9.20	240	3.61
10 vol% BTO-np	10.34	228	4.23
15 vol% BTO-np	12.73	218	3.56
20 vol% BTO-np	15.20	210	4.14
25 vol% BTO-np	17.70	205	3.46
30 vol% BTO-np	22.02	174	2.60
1 vol% BTO-nf	7.72	272	3.91
2 vol% BTO-nf	8.23	347	5.86
3 vol% BTO-nf	9.03	300	5.68
4 vol% BTO-nf	9.83	240	3.88
5 vol% BTO-nf	11.26	227	3.49

Based on these results, the composites with 2 vol% and 3 vol% of BTO-nf, which possess the highest E_b, were selected as the central layer to fabricate the topological structure modulated (TSM) nanocomposite films. BTO-np were introduced in the outer layers to induce high electric displacement. **Figure 2** presents the dielectric properties of TSM nanocomposite films as a function of frequency. The data show that the dielectric constant increases with the nanofillers loadings in both the outer layers and central layer, as expected. Dielectric relaxation is observed in all composites at frequency > 1 MHz, which is attributed to the frequency dispersion of the PVDF matrix. Moreover, except the dielectric relaxation (> 1 MHz), due to the PVDF matrix, the TSM nanocomposite films maintain a low dielectric loss at frequencies below 100 kHz.

The evolutions of the maximum of electric displacement and breakdown strength with the volume fractions of BTO-np and BTO-nf are presented in **Figure 3**. The most striking feature in Figure 3 is the simultaneously enhanced electric displacement and breakdown strength, as highlighted in the shaded area in the TSM nanocomposite films. Particularly, with 10 vol% of BTO-np in the BTO-np nanocomposite outer layers, the maximum electric displacement is increased from ~5.2 μC/cm^2 for 0 vol% to 6.0 μC/cm^2 for 2 vol% of BTO-nf, an enhancement of ~16%. Concomitantly, the breakdown strength is also enhanced by 67%, i.e., from ~228 kV/mm for 0 vol% to ~382 kV/mm for 2 vol% of BTO-nf. With the simultaneously enhanced E_b and *D*, the maximal U_{dis} of the multilayer composite with 10 vol% of BTO-np is significantly enhanced to 8.46 J/cm^3 which is larger than the maximal U_{dis} of 5.86 J/cm^3 for the BTO-nf/PVDF single layer films (see Table 1 and Figure S4 in the Supporting Information). A strong dependence of the maximal U_{dis} of the TSM nanocomposite films on the BTO-np concentration could also be observed in Figure S3 of Supporting Information, where

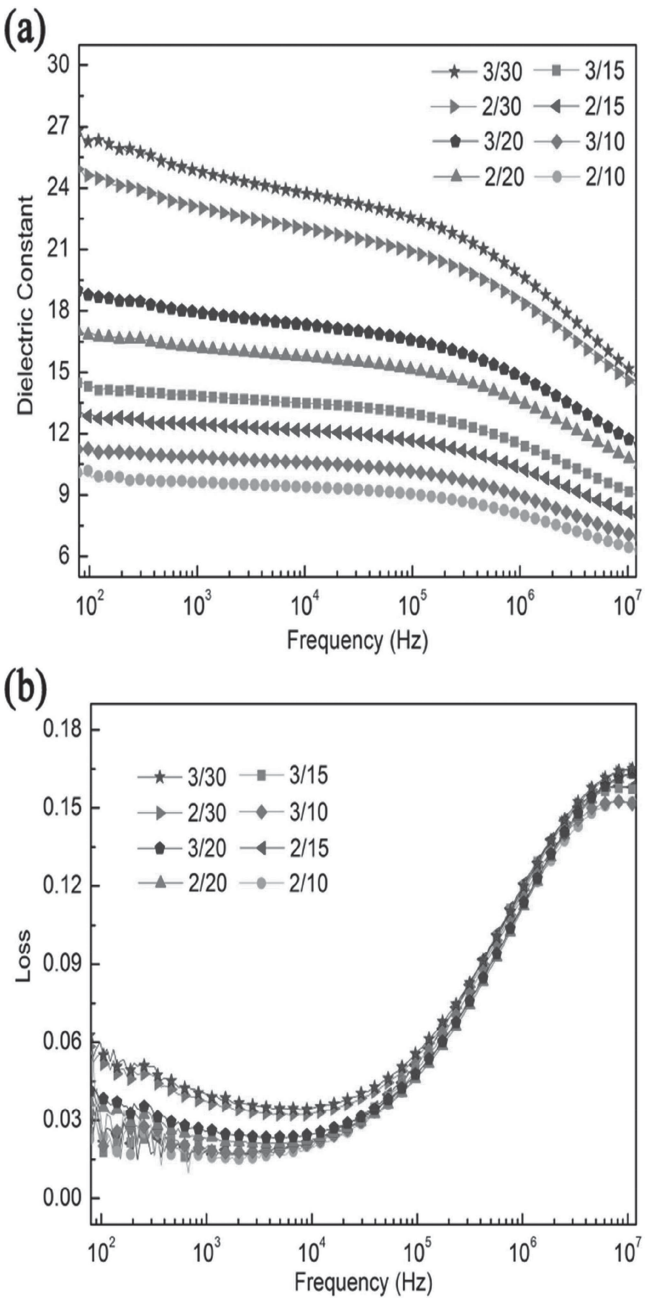

Figure 2. Frequency-dependent (a) dielectric constants (b) dielectric loss of the multilayer films. The labels show the nanofillers loadings in each composite, the number before the solidus reveals the BTO-nf loading (vol%) in the central layer and the number after the solidus reveals the BTO-np loading (vol%) in the outer layers.

the discharged energy density of the TSM nanocomposite films reaches a maximum at 10 vol% of BTO-np.

The experimental data further reveal the distinctive advantage of the TSM nanocomposite films in enhancing the dielectric breakdown compared with individual composite layers. With the same loading of BTO-nf, the breakdown strength of the TSM nanocomposite films can be even much higher than that of the single layer BTO-nf/PVDF composites, although in the multilayer composites the outer BTO-np/PVDF layers are

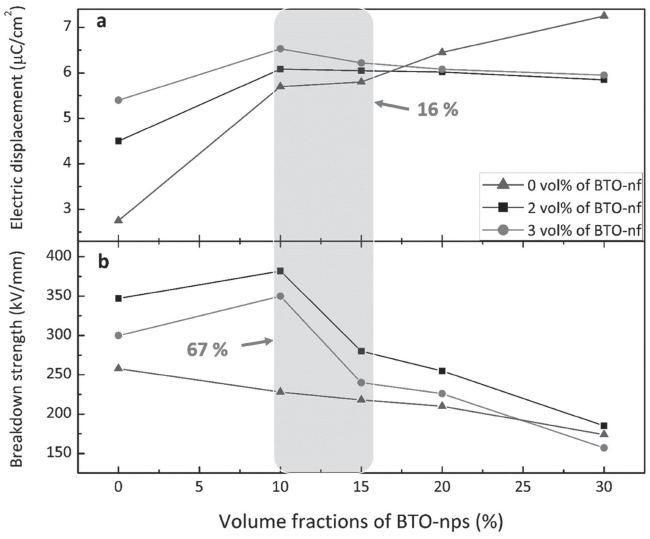

Figure 3. Variation of (a) maximal electric displacement and (b) breakdown strength of the multilayer composites with the volume fractions of BTO-np in the outer layers and BTO-nf in the central layers (2 vol%: square in black; 3 vol%: solid circle in red). Also superimposed are the data for the composites filled solely with BTO-np (denoted as 0 vol%: up-triangle in blue).

of much lower breakdown strength. For instance, the E_b of the BTO-nf/PVDF film with 2 vol% of BTO-nf is 347 kV/mm, while the E_b of the TSM nanocomposite films with 10 vol% of BTO-np is 382 kV/mm (see Table 1 and **Table 2** for C01–2). Further tailoring the thickness of the BTO-nf/PVDF central layers leads to even higher breakdown strength. With the fixed 2 vol% of BTO-nf in the central layer and 10 vol% of BTO-np in the outer layers, the TSM nanocomposite films were fabricated with the thickness of the central layer varying from 1 and 8 μm. As shown in **Figure 4**(a–d), the thickness of each layer were measured in the cross-sectional SEM images and listed in Table 2. Highest E_b of 453 kV/mm is achieved in C01–3 which has the central layer thickness ~3.5 μm. The TSM nanocomposite films with thinner or thicker central layer show lower breakdown strength than that of C01–3 while for the single layer of BTO-nf/PVDF composites no such a breakdown strength variation was observed. The results indicate that the enhanced breakdown strength is a unique feature of the TSM nanocomposite films. For a fixed thickness of the TSM nanocomposite films (~15 μm), variation of the central layer thickness could change the position of the interface between the neighboring layers. At the optimum interface position, the lengthening of the breakdown path may increase the propagation time of breakdown channel, leading to enhanced breakdown strength.

The significantly enhanced breakdown strength is also reflected by the fact that the optimized TSM nanocomposite films, the BTO-nf/PVDF layer can withstand much higher electric field before breakdown. Given the higher dielectric constants of the BTO-np/PVDF layers (ε_p = 10.3), higher electric field is concentrated in the BTO-nf/PVDF layer (ε_f = 8.2). Assuming the breakdown field is uniformly distributed in the TSM nanocomposite films, the breakdown fields in the BTO-np layers (E_p) and the BTO-nf layer (E_f) can be deduced from the model of capacitors in series, i.e., $E_p/E_f \propto \varepsilon_f/\varepsilon_p$. For

Table 2. The thickness of the layers and the performances of the sandwich films with 2 vol% BTO-nf loading in the central layer and 10 vol% BTO-np loading in the outer layers.

No.	Thickness of central layer (d_1) [μm]	Thickness of outer layers (d_2) [μm]	E_b [kV/mm]	U_{dis} [J/cm^3]	E_f^* [kV/mm]	E_p^* [kV/mm]
C01–1	1~2	7~8	311	6.32	382	304
C01–2	7~8	5~6	382	8.46	435	347
C01–3	3~4	5~6	453	9.72	511	407

Note: *local electric field determined by capacitive voltage divider as: $E_p = \frac{V}{2d_1 + \frac{\varepsilon_p}{\varepsilon_f} d_2}$, $E_f = \frac{V}{2d_1 + \frac{\varepsilon_f}{\varepsilon p} d_2}$, V: voltage applied; $\varepsilon_p = 10.3$, $\varepsilon_f = 8.2$: dielectric constants of the BTO-np and BTO-nf layers respectively.

instance, for C01–3 which has the highest breakdown strength of ~453 kV/mm, the breakdown field in the BTO-nf/PVDF layer thus obtained is ~511 kV/mm as compared with that of the BTO-nf/PVDF single layer composites (~347 kV/mm). As for the BTO-np/PVDF layer, E_p thus determined is ~407 kV/mm, which is enhanced by >80% over that of the BTO-np/PVDF single layer composites (~228 kV/mm, see in Table 1). Even for C01–1 with the lowest breakdown strength of ~311 kV/mm, the breakdown field in the BTO-np/PVDF layer is ~304 kV/mm, which is much higher than that of the BTO-np/PVDF single layer composites.

The significantly enhanced breakdown strength in these TSM composite films may be caused by several mechanisms. The redistribution of electric field among the different layers leads to local electric field much higher than its intrinsic breakdown strength in the BTO-np/PVDF layers, resulting in incomplete breakdown of the BTO-np/PVDF layer. Same incomplete breakdown has also been observed by Agoris et.al., in the three-layer polyethylene dielectrics,[26] where the Lichtenberg figure indicated that the incomplete breakdown channels were all contained in the central layer of higher dielectric constants. The electric energy accumulated in the BTO-np/PVDF layer can thus be liberated in the incomplete breakdown channels, which is favorable for the alleviation of the dielectric stress and avoids the complete breakdown of the multilayer composites.

With the same loading of BTO-np in the outer layers, the TSM nanocomposites films with central layers of different thickness exhibit mildly increased maximal electric displacement, i.e., from ~6.7 μC/cm^2 for C01–1 to ~7.0 μC/cm^2 for C01–3, while the breakdown strength increases significantly from ~311 kV/mm to ~453 kV/mm (see the *D-E* loops shown in Figure S4 in the Supporting Information). The remnant electric displacement (D_r) in the unipolar *D-E* loops, which is a sign of conduction loss, remains unchanged even under the much increased electric field in C01–3 (see also Figure S4). The discharged energy densities obtained from the *D-E* loops as a function of applied electric field amplitude are presented in **Figure 5**. In C01–3, a maximal U_{dis} of 9.7 J/cm^3 is obtained at ~453 kV/mm. For comparison, U_{dis} of BOPP, which is the

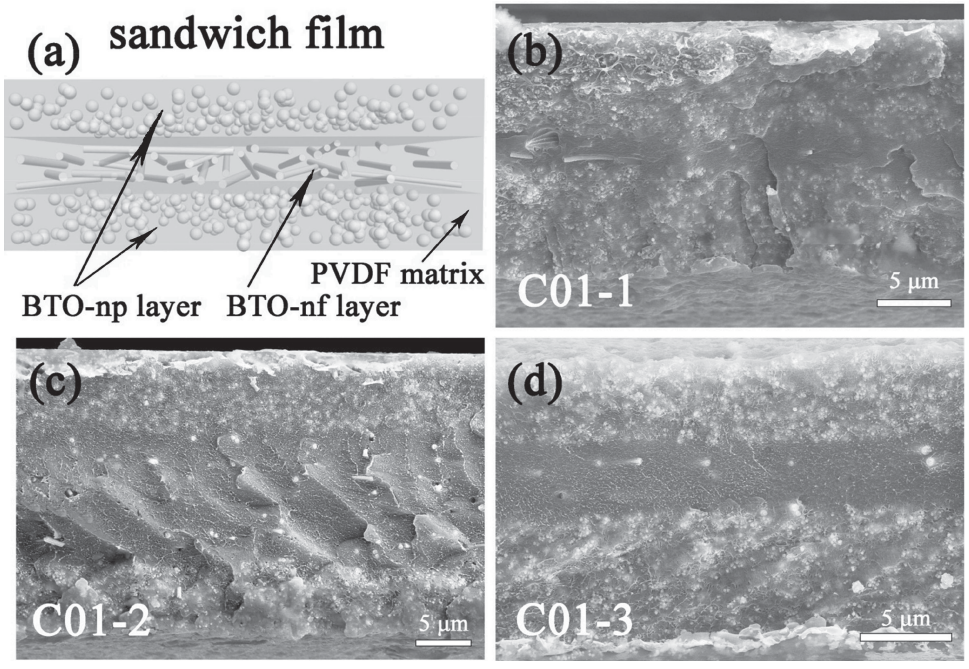

Figure 4. (a) A model of the sandwich-structured film with BTO-nf in the central layer and BTO-np in the outer layers. Cross-section SEM morphologies of the sandwich film (b) C01–1, (c) C01–2 and (d) C01–3.

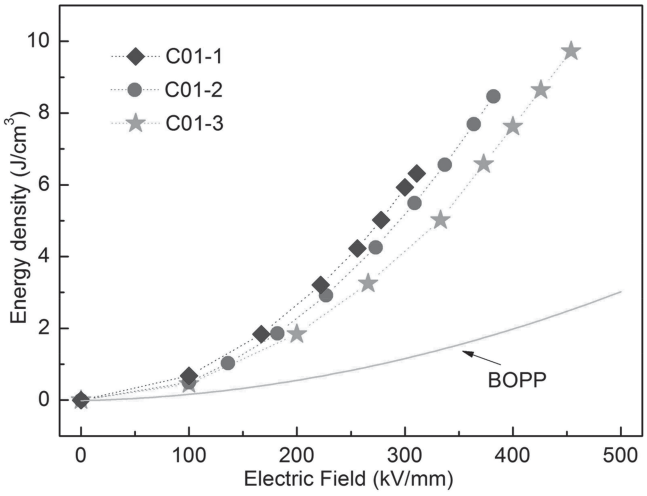

Figure 5. Electric field-dependent discharged energy densities of the multilayer films. For comparison, the energy densities of the BOPP is also included (data extrapolated from Ref. [25]).

bench mark dielectrics for energy storage applications, is ~2.3 J/cm^3 at the same electric field.

3. Conclusions

A class of topological structure modulated nanocomposite films was introduced that exhibit significantly enhanced dielectric strength and electric displacement compared with constitute composites and neat polymer films. The TSM nanocomposites films consist of a central BTO-nf/PVDF composite layer with the BTO-nf arranged in preferred orientations and two outer layers of BTO-np/PVDF nanocomposites. The preferred orientations of BTO-nfs (<4 vol%) in the PVDF matrix enhance the dielectric strength while the high volume loading BTO-np enhance dielectric constant compared with the PVDF matrix. As a result, the TSM nanocomposites films with the optimally tailored nano-morphology and topological structure exhibit discharged energy density of 9.72 J/cm^3 with a dielectric strength of 453 kV/mm. The results demonstrate the advantages of the TSM nanocomposite films that exhibit dielectric performance significantly exceeding the sum of the two constituents. Hence, these topological-structure modulated polymer nanocomposites provide a new and general approach for developing nanocomposite films with high energy density.

4. Experimental Section

Preparation of the Nanofillers: An electrospinning technique is employed to prepare $BaTiO_3$ nanofibers with high aspect ratios, using analytic grade reagents, barium acetate (99.0%, China National Chemicals Corporation Ltd.) and tetrabutyl titanate (98.0%, China National Chemicals Corporation Ltd.). The raw materials with target mol ratio were dissolved in acetic acid solvent, in which 1:2 mol ratio acetylacetone was dropped and stirred to get a homogeneous precursor solution. Poly(vinyl pyrrolidone) (PVP, M = 1 300 000) was added to control the solviscosity of the solution. The sol was then transferred into a syringe and electrospun with an applied electric field of 1.5 kV/cm. The electrospun fibers consisted of PVP and inorganic ions were treated at 700 °C for 3 h to get dense BTO ceramic nanofibers with diameters of 200–250 nm and lengths of 10–20 μm. Dopamine is used as the surface modification to improve the compatibility between the nanofiber fillers and the matrix.[27,28] The BTO nanofibers were ultrasonic dispersed in 0.01 mol/L of dopamine hydrochloride (99%, Alfa Aesar) aqueous solution and stirred for 12 h at 60 °C. The $BaTiO_3$ nanoparticles (99.9%) with an average particle size of 100 nm were purchased from Alfa Aesar, and were also modified by dopamine in aqueous solution.

Fabrication of the Nanocomposites: For the fabrication of the BTO-np/PVDF and the BTO-nf/PVDF single layer composite films, the dopamine-modified BTO-np or BTO-nf and PVDF powders were proportionally dispersed in *N,N*-dimethylformamide (DMF) by ultrasonication for 2 h, followed by stirring for 12 h, to form a stable suspension. The suspension was then cast into films by a laboratory casting equipment (LY-150–1, Beijing Orient Sun-Tec Company, Ltd.). The as-cast films were dried at 45 °C for 10 h for solvent volatilizing and the thickness of the final composite films was about 15 μm. The morphologies of the composites were observed by scanning electron microscopy (SEM, JSM-7001F, JEOL Ltd.). The multilayer films were cast layer by layer. For example, a part of the BTO-np/PVDF suspension was cast onto the tape and dried as an outer layer; then rewound the tape and casted the inner layer of the BTO-nf/PVDF; next, the rest of the BTO-np/PVDF suspension was cast onto the rewound tape as the other outer layer (See the schematic drawing in Figure 1); the multilayer film was finally dried at 45 °C for 10 h. The multilayer films thus obtained are ~15 μm in thickness. The cross-section morphology of the sandwich nanocomposite fabricated via layer by layer casting was observed by SEM.

Dielectric and Electrical Characterization: For electric measurement, copper electrodes of 60 nm in thickness were sputtered on both sides of the film samples using a mask with 3 mm diameter eyelets. The dielectric permittivity and the loss of the composite films were measured by a HP 4294A precision impedance analyzer (Agilent Technologies, Inc.) at room temperature. The *D-E* loops and the electric breakdown strengths of the composites were measured at 100 Hz by a Premier II ferroelectric test system (Radiant Technologies, Inc.) with a limited current of 1 mA.

Supporting Information

Supporting Information is available from the Wiley Online Library or from the author.

Acknowledgements

This work was supported by the NSF of China (Grant Nos. 51102142, 51222204, 50921061, 50903079), Specialized Research Fund for the Doctoral Program of Higher Education (Grant No.20110002120004), the Foundation for the Authors of National Excellent Doctoral Dissertations of China (Grant No.: 201144), Beijing Nova Program (Grant No.: XX2013037) and Tsinghua University (Grant No.20121087925).

Received: October 30, 2013
Revised: December 1, 2013
Published online: February 19, 2014

[1] a) B. J. Chu, X. Zhou, K. L. Ren, B. Neese, M. R. Lin, Q. Wang, F. Bauer, Q. M. Zhang, *Science* **2006**, *313*, 334; b) C. Baojin, Z. Xin, B. Neese, Q. M. Zhang, F. Bauer, *IEEE Trans. Dielectr. Electr. Insul.* **2006**, *13*, 1162.

[2] P. Barber, S. Balasubramanian, Y. Anguchamy, S. Gong, A. Wibowo, H. Gao, H. J. Ploehn, H. C. zur Loye, *Materials* **2009**, *2*, 1697.

[3] a) M. Rabuffi, G. Picci, *IEEE Trans. Plasma Sci.* **2002**, *30*, 1939; b) G. Picci, M. Rabuffi, *IEEE Trans. Plasma Sci.* **2000**, *28*, 1603.

[4] J. Ho, R. Ramprasad, S. Boggs, *IEEE Trans. Dielectr. Electr. Insul.* **2007**, *14*, 1295.
[5] T. C. M. Chung, *Green Sustainable Chem.* **2012**, *2*, 29.
[6] Y. Bai, Z. Y. Cheng, V. Bharti, H. S. Xu, Q. M. Zhang, *Appl. Phys. Lett.* **2000**, *76*, 3804.
[7] M. Arbatti, X. B. Shan, Z. Y. Cheng, *Adv. Mater.* **2007**, *19*, 1369.
[8] J. J. Li, J. Claude, L. E. Norena-Franco, S. Il Seok, Q. Wang, *Chem. Mater.* **2008**, *20*, 6304.
[9] L. Zhang, X. B. Shan, P. X. Wu, J. L. Song, Z. Y. Cheng, *Ferroelectr.* **2010**, *405*, 92.
[10] H. X. Tang, Y. R. Lin, C. Andrews, H. A. Sodano, *Nanotechnology* **2011**, 22.
[11] Q. Wang, L. Zhu, *J. Polym. Sci. Pt. B-Polym. Phys.* **2011**, *49*, 1421.
[12] Z. M. Dang, D. Xie, C. Y. Shi, *Appl. Phys. Lett.* **2007**, *91*, 222902.
[13] Y. Shen, Y. Lin, C.-W. Nan, *Adv. Funct. Mater.* **2007**, *17*, 2405.
[14] N. Guo, S. A. DiBenedetto, P. Tewari, M. T. Lanagan, M. A. Ratner, T. J. Marks, *Chem. Mater.* **2010**, *22*, 1567.
[15] J. Y. Li, L. Zhang, S. Ducharme, *Appl. Phys. Lett.* **2007**, *90*, 132901.
[16] P. Kim, N. M. Doss, J. P. Tillotson, P. J. Hotchkiss, M. J. Pan, S. R. Marder, J. Y. Li, J. P. Calame, J. W. Perry, *ACS Nano* **2009**, *3*, 2581.
[17] J. J. Li, S. I. Seok, B. J. Chu, F. Dogan, Q. M. Zhang, Q. Wang, *Adv. Mater.* **2009**, *21*, 217.
[18] T. Tanaka, M. Kozako, N. Fuse, Y. Ohki, *IEEE Trans. Dielectr. Electr. Insul.* **2005**, *12*, 669.
[19] a) L. A. Fredin, Z. Li, M. T. Lanagan, M. A. Ratner, T. J. Marks, *ACS Nano* **2013**, *7*, 396; b) L. A. Fredin, Z. Li, M. A. Ratner, M. T. Lanagan, T. J. Marks, *Adv. Mater.* **2012**, *24*, 5946; c) Z. Li, L. A. Fredin, P. Tewari, S. A. DiBenedetto, M. T. Lanagan, M. A. Ratner, T. J. Marks, *Chem. Mat.* **2010**, *22*, 5154.
[20] a) Y. U. Wang, *Appl. Phys. Lett.* **2010**, 96; b) Y. U. Wang, D. Q. Tan, *J. Appl. Phys.* **2011**, *109*, 104102.
[21] a) Y. Song, Y. Shen, H. Liu, Y. Lin, M. Li, C.-W. Nan, *J. Mater. Chem.* **2012**, *22*, 16491; b) Y. Song, Y. Shen, P. H. Hu, Y. H. Lin, M. Li, C. W. Nan, *Appl. Phys. Lett.* **2012**, *101*, 152904.
[22] A. B. Meddeb, Z. Ounaies, in Behavior and Mechanics of Multifunctional Materials and Composites 2012, Vol. *8342* (Eds: N. C. Goulbourne, Z. Ounaies), SPIE-Int Soc. Optical Engineering, Bellingham **2012**.
[23] a) H. X. Tang, H. A. Sodano, *Nano Lett.* **2013**, *13*, 1373; b) T. Haixiong, L. Yirong, H. A. Sodano, *Adv. Energy Mater.* **2013**, *3*, 451.
[24] a) V. Tomer, G. Polizos, C. A. Randall, E. Manias, *J. Appl. Phys.* **2011**, *109*, 074113; b) V. Tomer, E. Manias, C. A. Randall, *J. Appl. Phys.* **2011**, *110*, 044107; c) G. Polizos, V. Tomer, E. Manias, C. A. Randall, *J. Appl. Phys.* **2010**, *108*, 074117.
[25] a) T. J. Lewis, *J. Phys. D: Appl. Phys.* **2005**, *38*, 202; b) S. Wu, W. Li, M. Lin, Q. Burlingame, Q. Chen, A. Payzant, K. Xiao, Q. M. Zhang, *Adv. Mater.* **2013**, *25*, 1734.
[26] a) D. P. Agoris, I. Vitellas, O. S. Lebedev, Yu. P. Pokholkov, *J. Phys. D: Appl. Phys.* **2001**, *34*, 3485; b) L. A. Fredin, Z. Li, M. T. Lanagan, M. A. Ratner, T. J. Marks, *Adv. Funct. Mater.* **2013**, DOI: 10.1002/adfm.201202469.
[27] M. F. Lin, V. K. Thakur, E. J. Tan, P. S. Lee, *RSC Adv.* **2011**, *1*, 576.
[28] Y. Song, Y. Shen, H. Y. Liu, Y. H. Lin, M. Li, C. W. Nan, *J. Mater. Chem.* **2012**, *22*, 8063.